Biochemical and Biophysical Research Communications 511 (2019) 7–12

Contents lists available at ScienceDirect

Biochemical and Biophysical Research Communications

journal homepage: www.elsevier.com/locate/ybbrc

Ionic strength and calcium regulate membrane interactions of myelin basic protein and the cytoplasmic domain of myelin protein zero

Arne Raasakka [a], Nykola C. Jones [b], Søren Vrønning Hoffmann [b], Petri Kursula [a, c, *]

[a] Department of Biomedicine, University of Bergen, Bergen, Norway
[b] ISA, Department of Physics and Astronomy, Aarhus University, Aarhus, Denmark
[c] Faculty of Biochemistry and Molecular Medicine, University of Oulu, Oulu, Finland

ARTICLE INFO

Article history:
Received 1 February 2019
Accepted 5 February 2019
Available online 10 February 2019

Keywords:
Myelin basic protein
Protein zero
Intrinsic disorder
Protein folding
Lipid binding
Calcium

ABSTRACT

The formation of a mature myelin sheath in the vertebrate nervous system requires specific protein-membrane interactions. Several myelin-specific proteins are involved in stacking lipid membranes into multilayered structures around axons, and misregulation of these processes may contribute to chronic demyelinating diseases. Two key proteins in myelin membrane binding and stacking are the myelin basic protein (MBP) and protein zero (P0). Other factors, including Ca^{2+}, are important for the regulation of myelination. We studied the effects of ionic strength and Ca^{2+} on the membrane interactions of MBP and the cytoplasmic domain of P0 (P0ct). MBP and P0ct bound and aggregated negatively charged lipid vesicles, while simultaneously folding, and both ionic strength and calcium had systematic effects on these interactions. When decreasing membrane net negative charge, the level and kinetics of vesicle aggregation were affected by both salt and Ca^{2+}. The effects on lipid membrane surfaces by ions can directly affect myelin protein-membrane interactions, in addition to signalling effects in myelinating glia.

1. Introduction

Myelin contributes to the efficiency of both the central and peripheral nervous system (CNS and PNS, respectively) *via* axonal insulation and trophic support [1,2]. Comprised of tightly stacked lipid membranes held together by specific proteins, compact myelin (CM) – a water-deficient structure – insulates selected axonal segments and enables saltatory nerve impulse conduction. The ionic conditions in myelinating glia are fairly constant, with higher $[K^+]$ and $[Na^+]$ compared to neurons in general [3].

In myelinating glia, $[Ca^{2+}]$ and $[Zn^{2+}]$ (1 mM and 50 μM, respectively) are high compared to many other cell types [3,4], and Ca^{2+} signalling is important [5,6]. Due to the narrow spacing and low water content in CM, intracellular divalent cations must be subjects of attractive and repulsive interactions with phospholipid headgroups and myelin proteins. Intracellular Ca^{2+} levels have been linked to correct myelination [7–10].

Myelin basic protein (MBP) plays a fundamental role in forming and maintaining stable myelin, defining the boundaries between CM and non-compact myelin [11–13]. MBP is involved in multiple sclerosis (MS) [14,15], being an intrinsically disordered protein (IDP) that folds upon lipid binding [16–18]. MBP carries a positive charge and presents post-translationally citrullinated forms with differing net charge [19]. It requires negatively charged lipids for membrane adhesion, but correct myelin morphology also depends on other lipids and ions [10,18,20]. Binding of divalent cations to MBP [21–24] could, together with altered membrane compositions, influence its *in vivo* functions, having implications in MS and the stability of CM.

Myelin protein zero (P0) is a transmembrane protein in PNS myelin, relevant in human peripheral neuropathies and animal models [25,26]. P0 has an extracellular immunoglobulin-like domain, a single transmembrane helix, and a cytoplasmic tail (P0ct). Like MBP, P0ct is positively charged and interacts with phospholipids through electrostatics, gaining secondary structure [27,28]. This might make it susceptible to effects caused by cationic species.

We studied the effects of ionic strength and Ca^{2+} on the structural and functional aspects of MBP and P0ct binding to membranes using biophysical techniques. The results shed light on the interplay between ions and proteins in CM and support the role of Ca^{2+} [10,29,30] in regulating bilayer-MBP interactions.

* Corresponding author. Department of Biomedicine, University of Bergen, Bergen, Norway.
E-mail address: petri.kursula@uib.no (P. Kursula).

https://doi.org/10.1016/j.bbrc.2019.02.025
0006-291X/

2. Experimental procedures

2.1. Protein expression and purification

Mouse MBP and human P0ct were expressed and purified as described [18,28]. The final size-exclusion chromatography after affinity purification and tag removal was performed using Superdex75 16/60 HiLoad and Superdex75 increase 10/300 GL columns (GE Healthcare) in 20 mM HEPES, 150 mM NaCl, pH 7.5 (HBS). When required, the buffer was exchanged to water by sequential dialysis. Purified proteins were either used fresh or snap-frozen in liquid N_2 and stored at −80 °C.

2.2. Vesicle preparation

1,2-dimyristoyl-*sn*-glycero-3-phosphocholine (DMPC), 1,2-dimyristoyl-*sn*-glycero-3-phospho-(1′-rac-glycerol) (Na-salt) (DMPG), and the deuterated d_{54}-DMPC, d_{54}-DMPG, and d_7-cholesterol were from Avanti Polar Lipids (Alabaster, Alabama, USA). *n*-dodecylphosphocholine (DPC) was from Affymetrix.

Lipid stocks were prepared by dissolving dry lipids in chloroform or chloroform:methanol (9:1 v/v) at 10–30 mM. Mixtures were prepared at desired molar ratios, followed by solvent evaporation under N_2 and lyophilization. The dried lipids were stored airtight at −20 °C or used fresh for liposome preparation.

Liposomes were prepared by agitating dried lipids in water or HBS at 10–15 mM, followed by gentle mixing at ambient temperature, to ensure that no unsuspended lipids remained. Multilamellar vesicles were prepared by 7 freeze-thaw cycles using liquid N_2 and a warm water bath, with vortexing between. Small unilamellar vesicles (SUV) were prepared by sonicating fresh multilamellar vesicles using a probe tip sonicator (Materials Inc. Vibra-Cell VC-130) until clear, while avoiding overheating. All lipid preparations were immediately used for experiments.

2.3. Vesicle turbidimetry

For turbidimetric measurements, samples containing 0.5 mM DMPC:DMPG (1:1) SUVs with 2.5 μM P0ct or MBP were prepared in duplicate at 150 μl final volume on a Greiner 655161 96-well plate. Optical density at 450 nm was recorded immediately after thorough mixing at 25 °C using a Tecan Spark 20M plate reader.

2.4. Synchrotron radiation circular dichroism spectroscopy

SRCD data were collected from 0.1 to 0.4 mg ml^{-1} protein samples in water or 0.5% SDS on the AU-CD beamline at ASTRID2 (ISA, Aarhus, Denmark). Samples containing lipids were prepared immediately before measurement by mixing P0ct (P/L ratio 1:200) or MBP (P/L ratio 1:300) with freshly sonicated SUVs. 100-μm and 1-mm pathlength closed circular cells (Suprasil, Hellma Analytics) were used, and SRCD spectra were recorded from 170 to 280 nm at 30 °C. Data were processed using CDtoolX [31].

2.5. Stopped-flow SRCD

Rapid kinetic SRCD data were collected using an SX-20 stopped-flow instrument (Applied Photophysics) mounted on the AU-rSRCD branch line of the AU-AMO beamline at ASTRID2 (ISA, Aarhus, Denmark) at 30 °C. Acquisition of kinetic data comprised of 6–10 shots (160-μl total volume per shot) per sample. The two 1-ml syringes were loaded as follows: syringe 1 contained 0.1 mg ml^{-1} protein and syringe 2 a lipid solution (final molar P/L ratios of 1:200 and 1:300 for P0ct and MBP, respectively). The contents of each shot were rapidly mixed (2 ms dead time) before injection into the measurement cell (2-mm pathlength). CD signal was monitored at 195 nm for 5 s. Successful overlaying shots were averaged into a single curve for each sample. All sample sets were prepared and measured in duplicate. Water baselines were subtracted, and data were analyzed in GraphPad Prism 7 using single- and two-phase exponential decay functions to obtain rate constants.

3. Results

The folding and lipid membrane aggregation of MBP and P0ct were studied. Optical density measurements were used to observe the aggregation of lipid vesicles in the presence of proteins and different ions. The studies were expanded to different ratios of DMPC:DMPG, which affects the surface charge of the SUVs. Using SRCD, protein folding was probed, and time-resolved experiments provided data on membrane aggregation kinetics.

3.1. The effect of ionic content on myelin protein-induced vesicle turbidity

As a functional assay for MBP and P0ct, turbidimetric experiments on SUVs were carried out. In our earlier studies, we concluded that in the presence of MBP, net negatively charged lipid vesicles aggregate and subsequently form myelin-like bilayer stacks, resulting in sample turbidity [18]. P0ct, on the other hand, can cause SUVs to undergo fusion events to produce large aggregated lipid bodies [28], which may cause additional sample turbidity.

The turbidity induced by the proteins for 1:1, 4:1, and 9:1 DMPC:DMPG SUVs, at a 1:200 protein-to-lipid (P/L) ratio, was determined. The experiments were carried out at various concentrations of NaCl, NaF, and $CaCl_2$. Since especially multivalent cations may induce lipid aggregation in the absence of proteins [32], control samples without proteins were included (Fig. 1). Protein-free sample turbidity was observed mostly in the presence of $CaCl_2$, with more $CaCl_2$ needed for induction, when the lipids became more negatively charged. The effect of monovalent ions as inducers of turbidity *per se* in protein-free samples was low.

The turbidity induced by MBP was higher than that of P0ct, with the exception of DMPC:DMPG (9:1), in which P0ct was more efficient than MBP. In the presence of either protein, the induced turbidity systematically increased with salt concentration in DMPC:DMPG (1:1) (Fig. 1A). In DMPC:DMPG (4:1) and (9:1), the turbidity decreased above a certain ionic strength (Fig. 1B and C), and the balance between ionic strength and lipid net charge plays a role in protein-induced membrane aggregation. The turbidification of DMPC:DMPG (9:1) was abolished at salt concentrations of 150 mM or above. In all lipid mixtures, both proteins in the presence of NaCl and NaF produced roughly the same levels of turbidity and concentration-dependent trends. Thus, the choice of monovalent anion matters little in the level of induced turbidity.

To mimic the physiological concentration, $CaCl_2$ was included at much lower concentration than NaCl and NaF, but increased turbidity was still observed. $CaCl_2$ induced lipid turbidity in the absence of protein; the levels varied as a function of concentration. Calcium-induced turbidity showed differences between the three DMPC:DMPG ratios: the turbidification of DMPC:DMPG (1:1) vesicles was more resistant to $CaCl_2$ than 4:1 and 9:1 mixtures (Fig. 1).

$CaCl_2$ changed the turbidity induced by MBP and P0ct, depending on the membrane composition. In DMPC:DMPG (1:1), turbidity was highest, at a similar level to that induced by the presence of salt (Fig. 1A). DMPC:DMPG (9:1) showed least turbidity, and high calcium concentrations brought it to baseline levels (Fig. 1C). Interestingly, in DMPC:DMPG (4:1), 0.5 mM and 1 mM $CaCl_2$ showed a large difference in turbidity in the absence of

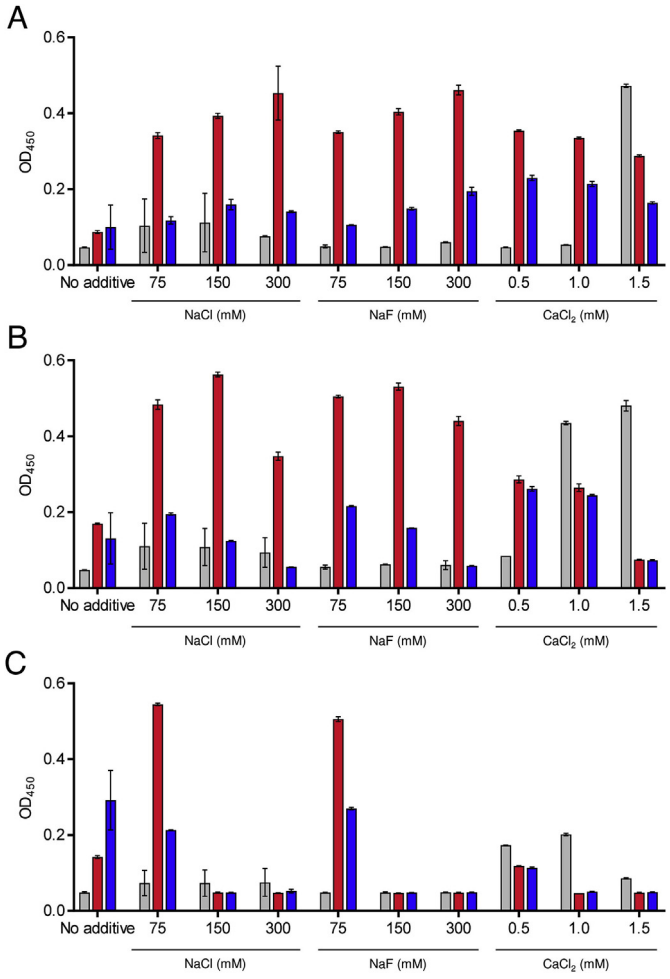

Fig. 1. Vesicle turbidimetry. MBP (red) and P0ct (blue)-induced turbidity was studied in (A) 1:1, (B) 4:1, and (C) 9:1 DMPC:DMPG under different salt conditions. Absence of protein, gray. Error bars represent standard deviation. (For interpretation of the references to colour in this figure legend, the reader is referred to the Web version of this article.)

proteins, but when proteins were included, the levels were almost identical, indicating that the proteins could override the effect of $CaCl_2$ at moderate concentrations (Fig. 1B). 1.5 mM $CaCl_2$ decreased the turbidity induced by MBP or P0ct in all membrane compositions. Thus, while salt can influence the interactions between proteins and lipids, and protein-decorated vesicles with each other, the effect of Ca^{2+} with phospholipid headgroups is rather specific. Even small changes in Ca^{2+} levels, in the range 0.5–1.5 mM, can alter the protein-lipid interactions required for vesicle aggregation and fusion, given that negatively charged lipid species are not predominant.

3.2. Folding of lipid-bound MBP and P0ct

We earlier observed lipid-induced increase in secondary structure for MBP and P0ct in the absence of salt [18,28]. To investigate the effect of ionic strength and divalent cations on folding, SRCD was carried out with 150 mM NaF and 1 mM $CaCl_2$. NaF was used due to the high UV absorbance of Cl^-. NaF had a very similar behaviour to NaCl in turbidimetry (Fig. 1).

NaF and $CaCl_2$ had no effect on MBP or P0ct folding in water or 0.5% SDS (Supplementary Fig. S1). SRCD spectra for proteins in the presence of lipids often suffer from turbidity-induced light scattering - here, especially at 1:1 and 4:1 DMPC:DMPG ratios with $CaCl_2$ (Fig. 2A and B). Under such conditions, the positions of the spectral peaks can be used to detect the presence of secondary structure. The observed changes in conformation correspond well to the turbidimetry assays under the same conditions, whereby the negative peak at 200 nm indicates unfolded structure and possibly lack of membrane binding.

MBP reached a similar secondary structure content in all lipid compositions (Fig. 2). In DMPC:DMPG (9:1), NaF and $CaCl_2$ decreased MBP helical content, potentially indicating less binding to lipids (Fig. 2C). Also P0ct obtained secondary structure in lipid mixtures, and the decrease of membrane negative charge (DMPG) correlated with the loss of P0ct helical structure - seen as the movement of the main minimum towards 200 nm (Fig. 2). NaF had a small unfolding effect on P0ct in all lipid mixtures.

3.3. The kinetics of initial vesicle nucleation

To visualize the kinetics of MBP and P0ct binding to lipid vesicles, stopped-flow SRCD measurements were carried out. The original goal was to study protein folding kinetics when encountering lipid membranes, but initial measurements and optimization revealed that the proteins gained their folding completely within the instrument dead time (~2 ms), making the kinetics practically impossible to follow.

Despite the setback with folding kinetics, a strong decay in SRCD signal was observed within a 5–10 s measurement window (before the onset of induced photodegradation), when proteins were mixed with lipids in the presence of 150 mM NaF or 1 mM $CaCl_2$ (Fig. 3A). This resembled exponential decay and could be described with two potentially independent rate constants (Supplementary Table 1). Since we observed similar behaviour in the absence of proteins (Supplementary Fig. S2, Supplementary Table 1), the effect does not involve protein folding. Considering the wavelength of the beam (195 nm), in the size range of large vesicular lipid bodies, and decay strength (tens of mdeg), the effect is caused by light scattering from vesicle fusion and/or aggregation, especially since the lipid mixtures and ionic conditions correlate with the observed steady states in turbidimetry (Fig. 1).

While lipids mixed with $CaCl_2$ alone produced quite noisy data with individual shots and replicates not overlaying very well, all protein samples had excellent reproducibility both in terms of shot quality and between replicates, which is evident from the small standard deviations. The data could be fitted with confidence, and in most cases, two rate constants were obtained: k_1, which describes a fast event (>2 s^{-1}), and k_2, for a slower event (<1 s^{-1}). The rate constants in the presence of proteins vary between lipid compositions (Fig. 3B). The accuracy of k_2 is rather low, given the limited time window of the experiments.

In the absence of proteins, the turbidity kinetics induced by Ca^{2+} were similar in DMPC:DMPG (4:1) and (9:1), and slower in DMPC:DMPG (1:1) (Supplementary Fig. S2, Supplementary Table 1), suggesting a role for electrostatic repulsion. As the two less charged lipid compositions aggregate with roughly the same rate, the effect is likely to occur due to saturation of the surface with Ca^{2+}. The concentration of $CaCl_2$ in these experiments was 1 mM, while the total concentration of lipid negative headgroups was either 0.25, 0.1, or 0.05 mM. It appears that the membranes with less charge are fully neutralized, while the neutralization might be partial for the 1:1 mixture.

In protein-lipid samples, in the presence of NaF and $CaCl_2$, DMPC:DMPG (1:1) presents a higher k_1 than the other two lipid compositions. The effects of the two salts on k_1 increase with the molar percentage of DMPG (Fig. 3B, Supplementary Table 1).

In DMPC:DMPG (9:1), the aggregation effect was dominated by

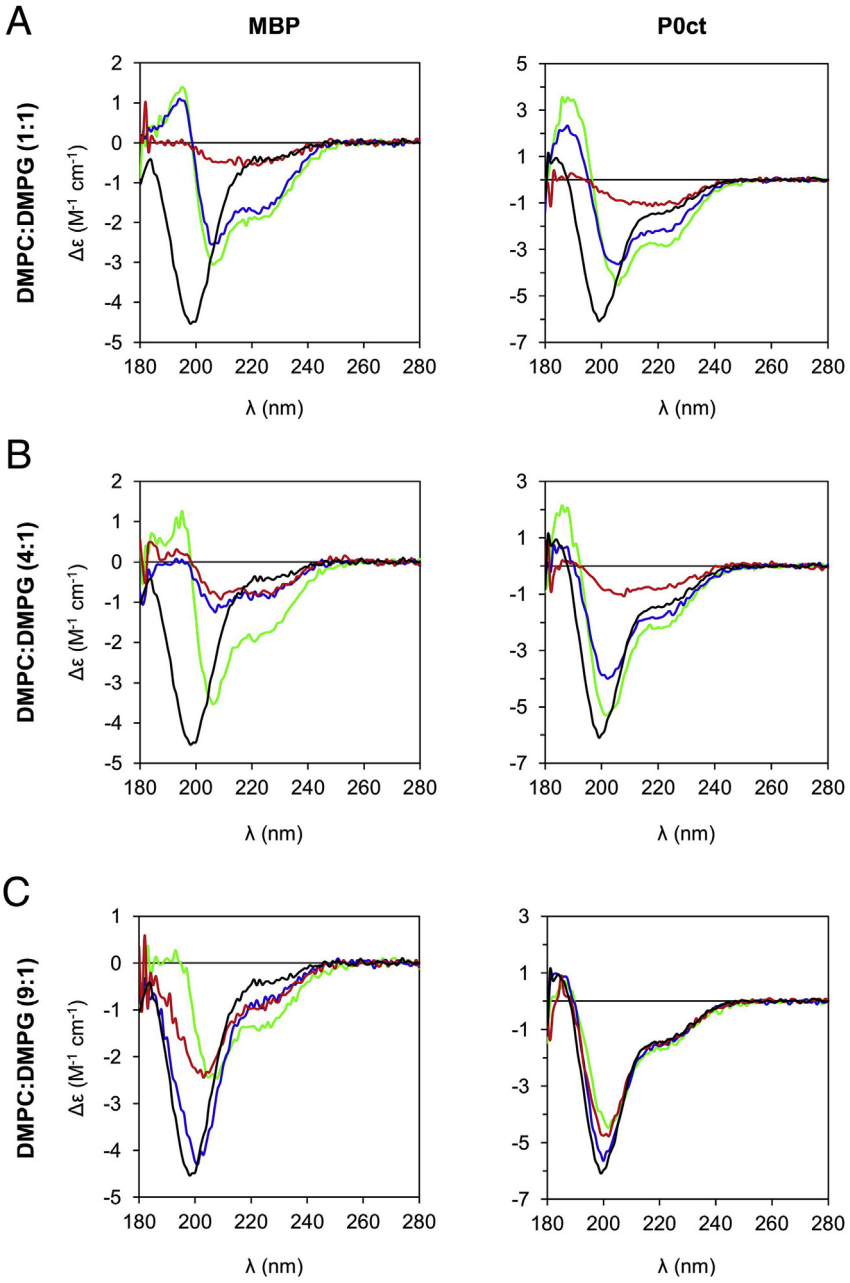

Fig. 2. Lipid-induced protein folding. Three ratios of DMPC:DMPG were used: 1:1 (A), 4:1 (B), and 9:1 (C). No additive, green; 150 mM NaF, blue; 1 mM $CaCl_2$, red. Protein controls in water (black) are plotted for reference. (For interpretation of the references to colour in this figure legend, the reader is referred to the Web version of this article.)

the 1 mM $CaCl_2$ over proteins (Supplementary Table 1); this correlates with steady-state turbidity (Fig. 1C). The rate constants are similar regardless of the presence of protein, indicating that the aggregation under this condition is governed by the cation. On the other hand, 150 mM NaF inhibits aggregation of DMPC:DMPG (9:1) vesicles (Fig. 1C, Supplementary Table 1), and in salt-free conditions, the proteins display aggregation, which was not the case for the other two vesicle compositions (Fig. 3A). Taken together, the kinetics correlate well with turbidimetry, providing insights into determinants of membrane binding and stacking.

4. Discussion

Myelination requires a balance between myelin protein expression, protein-membrane interactions, and regulatory factors, such as calcium. Both MBP and P0ct are IDPs in solution, but upon binding to membranes, they fold into helical structures, altering the physical properties of the membrane [13,17,18,28,33]. The salt sensitivity of the protein-membrane interactions supports the role of electrostatic interactions in them, and the effects of calcium on the molecular interactions indicate more specific regulation.

Phospholipid vesicle aggregation was followed to see how salt content and Ca^{2+} influence the activity and folding of MBP and P0ct. Our results show that while vesicle turbidity increases with ionic strength, both in the steady state and in initial kinetics, the effect of salt varies with membrane surface net charge. Considering the combination of ionic strength and membrane charge, high salt concentrations effectively screen the protein-membrane interactions, while lower concentrations, in fact, have an inducing effect. The results are in line with extractability of MBP from myelin

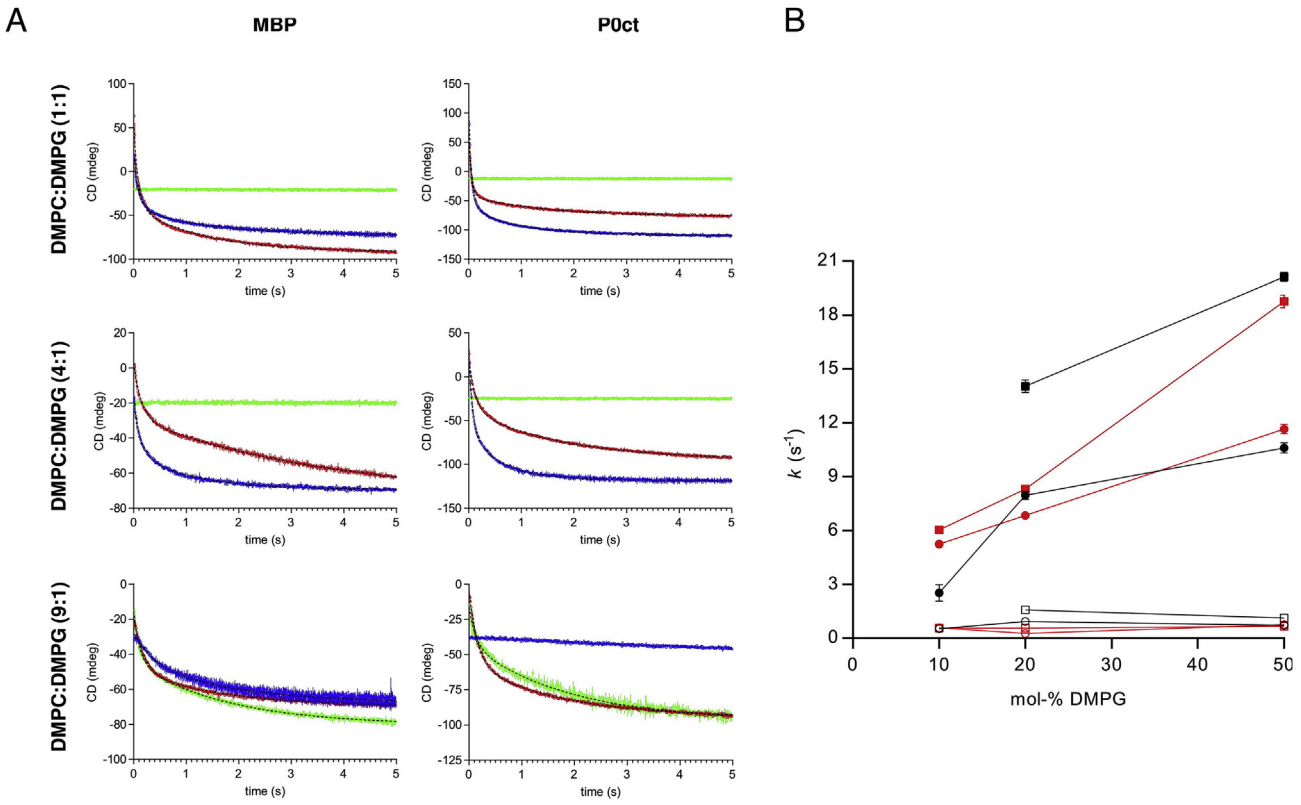

Fig. 3. Rapid kinetics of protein-induced lipid turbidity. A. SRCD was monitored at 195 nm for 5 s. Proteins were mixed with lipids in the absence (green) and presence of 150 mM NaF (blue) or 1 mM $CaCl_2$ (red). Fits (dashed black) are shown where data fitting was successful. B. Comparison of kinetic parameters. Rate constants (k_1, solid; k_2, open) as a function of DMPG fraction in 150 mM NaF (black) and 1 mM $CaCl_2$ (red). Circles, MBP; squares, P0ct. Error bars represent standard deviation. (For interpretation of the references to colour in this figure legend, the reader is referred to the Web version of this article.)

and myelin swelling under different conditions [34–36].

The effects of calcium are likely to be more specific than the electrostatic competition caused by near-physiological ionic strength *per se*. Ca^{2+} alone induces spontaneous vesicle turbidity, showing that it affects the surface properties of the membrane. Calcium influences both the steady-state levels and the kinetics of MBP- and P0ct-mediated vesicle aggregation. The binding of divalent cations by MBP has been observed in earlier studies [21–23], and calcium affects both MBP solubility in purified myelin as well as myelin membrane spacing [36,37]. It, thus, appears that calcium might be able to affect the surface of both the protein and the membrane in a manner that can regulate the direct molecular interaction.

Time-resolved SRCD was used to follow the kinetics of vesicle aggregation. While it is at the moment unclear what the rate constants represent, the observed kinetics may be relevant to myelin membrane stacking. Considering the k_1 values, P0ct is faster than MBP at inducing turbidity. The difference could arise from the smaller size of P0ct, which potentially tumbles in solution faster than MBP and folds more easily onto membranes. Being larger, MBP experiences more steric and repulsive effects from proteins already on the membrane.

Several studies have highlighted calcium as a regulator of proper myelination [5,7,8,30,38], and in addition to being crucial for signalling and cellular homeostasis, it has been suggested to directly affect MBP-membrane interactions [10,30,36]. Phosphoinositides are important constituents of myelin, involved in MBP-membrane interactions regulated by Ca^{2+} [30]. Various mechanisms have been proposed for the effects of calcium on myelin structure and formation; these include activation of calpains, the involvement of calmodulin, signalling pathways, cytoskeletal events, and effects on protein-lipid interactions [5,7–10,30].

It was proposed that a “sweet spot” concentration of calcium exists during normal myelination [9]. Deviations from this range might be relevant for dys/demyelination. Similar effects were observed in early studies on MBP extraction from nerve tissue [29,36]. Here, concentrations around the physiological [Ca^{2+}] were used to follow myelin protein-membrane interactions, and concentration dependence around 1 mM [Ca^{2+}] is evident. Together with the membrane surface charge, calcium may either promote or inhibit lipid membrane stacking induced by myelin proteins. The obvious next steps involve studies on the effects of calcium on myelin protein-membrane interactions in more physiological lipid compositions corresponding to the myelin cytoplasmic leaflet; the experiments here using simplified lipid mixtures pave the way for these studies.

MBP and P0 are not related by sequence; however, the physicochemical properties of MBP and P0ct are similar [13,17,18,27,28,33]. Both bind to membrane surfaces through electrostatic interactions, get embedded and fold, and affect properties of the lipid bilayer. Functional similarity extends to the effects of ionic strength and calcium. Our observations point towards common regulatory mechanisms for myelin proteins during myelin maturation and maintenance.

Author contributions

Study design, original text and figures: A.R., P.K.
Prepared samples and performed experiments: A.R.
Processed and analyzed data: A.R., N.C.J., S.V.H., P.K.

Review & editing: A.R., N.C.J., S.V.H, P.K.
Supervision: P.K.

Competing financial interests

The authors declare no competing financial interests.

Data availability

The datasets generated and analyzed during the current study are available from the corresponding author on reasonable request.

Acknowledgements

This work was supported by the Norwegian Research Council (SYNKNØYT programme). We acknowledge the ASTRID2 synchrotron facility and the BiSS facility at the University of Bergen. This research was supported by the project CALIPSOplus under the Grant Agreement 730872 from the EU Framework Programme for Research and Innovation HORIZON 2020.

Transparency document

Transparency document related to this article can be found online at https://doi.org/10.1016/j.bbrc.2019.02.025.

Appendix A. Supplementary data

Supplementary data to this article can be found online at https://doi.org/10.1016/j.bbrc.2019.02.025.

References

[1] D.K. Hartline, What is myelin? Neuron Glia Biol. 4 (2008) 153–163.
[2] K.A. Nave, Myelination and the trophic support of long axons, Nat. Rev. Neurosci. 11 (2010) 275–283.
[3] P.K. Stys, E. Lehning, A.J. Saubermann, R.M. LoPachin, Intracellular concentrations of major ions in rat myelinated axons and glia: calculations based on electron probe X-ray microanalyses, J. Neurochem. 68 (1997) 1920–1928.
[4] J.M. Bourre, I. Cloez, M. Galliot, A. Buisine, O. Dumont, M. Piciotti, F. Prouillet, R. Bourdon, Occurrence of manganese, copper and zinc in myelin. Alterations in the peripheral nervous system of dysmyelinating trembler mutant are at variance with brain mutants (quaking and shiverer), Neurochem. Int. 10 (1987) 281–286.
[5] M. Friess, J. Hammann, P. Unichenko, H.J. Luhmann, R. White, S. Kirischuk, Intracellular ion signaling influences myelin basic protein synthesis in oligodendrocyte precursor cells, Cell Calcium 60 (2016) 322–330.
[6] L.L. Haak, M. Grimaldi, J.T. Russell, Mitochondria in myelinating cells: calcium signaling in oligodendrocyte precursor cells, Cell Calcium 28 (2000) 297–306.
[7] M. Baraban, S. Koudelka, D.A. Lyons, Ca $^{2+}$ activity signatures of myelin sheath formation and growth in vivo, Nat. Neurosci. 21 (2018) 19–23.
[8] A.M. Krasnow, M.C. Ford, L.E. Valdivia, S.W. Wilson, D. Attwell, Regulation of developing myelin sheath elongation by oligodendrocyte calcium transients in vivo, Nat. Neurosci. 21 (2018) 24–28.
[9] R.H. Miller, Calcium control of myelin sheath growth, Nat. Neurosci. 21 (2018) 2–3.
[10] M.T. Weil, W. Möbius, A. Winkler, T. Ruhwedel, C. Wrzos, E. Romanelli, J.L. Bennett, L. Enz, N. Goebels, K.A. Nave, M. Kerschensteiner, N. Schaeren-Wiemers, C. Stadelmann, M. Simons, Loss of myelin basic protein function triggers myelin breakdown in models of demyelinating diseases, Cell Rep. 16 (2016) 314–322.
[11] S. Aggarwal, N. Snaidero, G. Pähler, S. Frey, P. Sánchez, M. Zweckstetter, A. Janshoff, A. Schneider, M.T. Weil, I.A. Schaap, D. Görlich, M. Simons, Myelin membrane assembly is driven by a phase transition of myelin basic proteins into a cohesive protein meshwork, PLoS Biol. 11 (2013), e1001577.
[12] N. Snaidero, C. Velte, M. Myllykoski, A. Raasakka, A. Ignatev, H.B. Werner, M.S. Erwig, W. Möbius, P. Kursula, K.A. Nave, M. Simons, Antagonistic functions of MBP and CNP establish cytosolic channels in CNS myelin, Cell Rep. 18 (2017) 314–323.
[13] K.A. Vassall, V.V. Bamm, G. Harauz, MyelStones: the executive roles of myelin basic protein in myelin assembly and destabilization in multiple sclerosis, Biochem. J. 472 (2015) 17–32.
[14] Y. Li, Y. Huang, J. Lue, J.A. Quandt, R. Martin, R.A. Mariuzza, Structure of a human autoimmune TCR bound to a myelin basic protein self-peptide and a multiple sclerosis-associated MHC class II molecule, EMBO J. 24 (2005) 2968–2979.
[15] M. Sospedra, R. Martin, Immunology of multiple sclerosis, Semin. Neurol. 36 (2016) 115–127.
[16] G.L. Mendz, D.J. Miller, G.B. Ralston, Interactions of myelin basic protein with palmitoyllysophosphatidylcholine: characterization of the complexes and conformations of the protein, Eur. Biophys. J. 24 (1995) 39–53.
[17] E. Polverini, A. Fasano, F. Zito, P. Riccio, P. Cavatorta, Conformation of bovine myelin basic protein purified with bound lipids, Eur. Biophys. J. 28 (1999) 351–355.
[18] A. Raasakka, S. Ruskamo, J. Kowal, R. Barker, A. Baumann, A. Martel, J. Tuusa, M. Myllykoski, J. Bürck, A.S. Ulrich, H. Stahlberg, P. Kursula, Membrane association landscape of myelin basic protein portrays formation of the myelin major dense line, Sci. Rep. 7 (2017) 4974.
[19] G. Harauz, A.A. Musse, A tale of two citrullines–structural and functional aspects of myelin basic protein deimination in health and disease, Neurochem. Res. 32 (2007) 137–158.
[20] K. Widder, J. Träger, A. Kerth, G. Harauz, D. Hinderberger, Interaction of myelin basic protein with myelin-like lipid monolayers at air-water interface, Langmuir 34 (2018) 6095–6108.
[21] C. Baran, G.S. Smith, V.V. Bamm, G. Harauz, J.S. Lee, Divalent cations induce a compaction of intrinsically disordered myelin basic protein, Biochem. Biophys. Res. Commun. 391 (2010) 224–229.
[22] P. Riccio, S. Giovannelli, A. Bobba, E. Romito, A. Fasano, T. Bleve-Zacheo, R. Favilla, E. Quagliariello, P. Cavatorta, Specificity of zinc binding to myelin basic protein, Neurochem. Res. 20 (1995) 1107–1113.
[23] G.S. Smith, L. Chen, V.V. Bamm, J.R. Dutcher, G. Harauz, The interaction of zinc with membrane-associated 18.5 kDa myelin basic protein: an attenuated total reflectance-Fourier transform infrared spectroscopic study, Amino Acids 39 (2010) 739–750.
[24] D. Tsang, Y.S. Tsang, W.K. Ho, R.N. Wong, Myelin basic protein is a zinc-binding protein in brain: possible role in myelin compaction, Neurochem. Res. 22 (1997) 811–819.
[25] J. de Sèze, L. Kremer, C. Alves do Rego, O. Taleb, D. Lam, W. Beiano, G. Mensah-Nyagan, E. Trifilieff, S. Brun, Chronic inflammatory demyelinating polyradiculoneuropathy: a new animal model for new therapeutic targets, Rev. Neurol. (Paris) 172 (2016) 767–769.
[26] M.E. Shy, A. Jáni, K. Krajewski, M. Grandis, R.A. Lewis, J. Li, R.R. Shy, J. Balsamo, J. Lilien, J.Y. Garbern, J. Kamholz, Phenotypic clustering in MPZ mutations, Brain 127 (2004) 371–384.
[27] X. Luo, D. Sharma, H. Inouye, D. Lee, R.L. Avila, M. Salmona, D.A. Kirschner, Cytoplasmic domain of human myelin protein zero likely folded as beta-structure in compact myelin, Biophys. J. 92 (2007) 1585–1597.
[28] A. Raasakka, S. Ruskamo, J. Kowal, H. Han, A. Baumann, M. Myllykoski, A. Fasano, R. Rossano, P. Riccio, J. Bürck, A.S. Ulrich, H. Stahlberg, P. Kursula, Molecular structure and function of myelin protein P0 in membrane stacking, Sci. Rep. 9 (2019) 642.
[29] P. Glynn, A. Chantry, N. Groome, M.L. Cuzner, Basic protein dissociating from myelin membranes at physiological ionic strength and pH is cleaved into three major fragments, J. Neurochem. 48 (1987) 752–759.
[30] S. Nawaz, A. Kippert, A.S. Saab, H.B. Werner, T. Lang, K.A. Nave, M. Simons, Phosphatidylinositol 4,5-bisphosphate-dependent interaction of myelin basic protein with the plasma membrane in oligodendroglial cells and its rapid perturbation by elevated calcium, J. Neurosci. 29 (2009) 4794–4807.
[31] A.J. Miles, B.A. Wallace, CDtoolX, a downloadable software package for processing and analyses of circular dichroism spectroscopic data, Protein Sci. 27 (2018) 1717–1722.
[32] S. Ohki, N. Düzgüneş, K. Leonards, Phospholipid vesicle aggregation: effect of monovalent and divalent ions, Biochemistry 21 (1982) 2127–2133.
[33] C. Wang, U. Neugebauer, J. Bürck, M. Myllykoski, P. Baumgärtel, J. Popp, P. Kursula, Charge isomers of myelin basic protein: structure and interactions with membranes, nucleotide analogues, and calmodulin, PLoS One 6 (2011), e19915.
[34] D.L. Caspar, V. Melchior, C.J. Hollingshead, D.A. Kirschner, Dynamics of myelin membrane contacts, Soc. Gen. Physiol. 34 (1980) 195–211.
[35] C.J. Hollingshead, D.L. Caspar, V. Melchior, D.A. Kirschner, Compaction and particle segregation in myelin membrane arrays, J. Cell Biol. 89 (1981) 631–644.
[36] D. Johnson, R. Toms, H. Weiner, Studies of myelin breakdown in vitro, in: S.U. Kim (Ed.), Myelination and Demyelination - Implications for Multiple Sclerosis, 1989, pp. 219–236.
[37] R. Padrón, L. Mateu, D.A. Kirschner, X-ray diffraction study of the kinetics of myelin lattice swelling. Effect of divalent cations, Biophys. J. 28 (1979) 231–239.
[38] V.T. Cheli, D.A. Santiago González, T. Namgyal Lama, V. Spreuer, V. Handley, G.G. Murphy, P.M. Paez, Conditional deletion of the L-type calcium channel Cav1.2 in oligodendrocyte progenitor cells affects postnatal myelination in mice, J. Neurosci. 36 (2016) 10853–10869.